Journal of Control, Automation and Electrical Systems (2022) 33:1724–1738
https://doi.org/10.1007/s40313-022-00937-8

Technical–Economic Evaluation of EV Fast Charging Station with Distributed Energy Resources

Bruno P. Cancian[1] · **José C. G. Andrade**[1] · **Walmir Freitas**[1]

Received: 15 September 2021 / Revised: 19 May 2022 / Accepted: 16 July 2022 / Published online: 11 August 2022

Abstract
Over the last decade, the electrification of the transportation fleet emerged as a solution to reduce climate change. To electric vehicles (EVs) become widespread, charging stations must be deployed, especially fast stations (FCSs), to allow over-ranged travel. Previous works have analyzed the technical impacts of FCSs, also in combination with photovoltaic (PV) and battery energy storage system (BESS); however, a combined stochastic technical–economic evaluation has been less discussed. The objective of this work is to develop a technical–economic method to determine: (i) the most profitable time-of-use electricity tariff for a charging station; and (ii) the economic feasibility of PVs and BESS integration with FCSs and how these technologies affect the overall profitability. A real Brazilian distribution system is used as a case study, considering local time-of-use tariffs for low (LV) and medium (MV) voltage customers. Technical results show that PVs and BESSs can reduce 4–7% voltage problems; however, may increase overload issues, especially in LV connection. From the economic perspective, MV connections have higher profits using Blue tariff instead of Green, while LV connections are preferred with the Conventional tariff. Also, PVs are cost-effective equipment to be added to the charging station, while storages are only profitable if they only use the PV energy generated to supply the EVs, *i.e.*, a low daily number of EVs charging in the FCS.

Keywords Battery energy storage system · Charging station · Distribution system · Electric vehicle · Solar photovoltaic generation

1 Introduction

Over the last decades, the need to reduce CO_2 emissions has gained attention on a global scale due to the consequences of climate change. Almost 25% of all CO_2 emitted to the atmosphere comes from internal combustion engine vehicles, 75% of this amount comes from road vehicles, in its majority traveling vehicles (IEA, 2020). As a consequence of this scenario, the biggest global economies have begun investing in the development of electric vehicles (EVs). It is forecast that 7–12% of the global vehicle fleet will correspond to EVs by 2030 depending on the incentives given (IEA, 2021). In the Brazilian case, it is estimated that EVs will represent 62% of the market share (new sales) and 18% of the fleet by 2035 (ANFAVEA, 2021).

The EV penetration growth increases the demand for EVs charging stations (CSs); in this manner, are expected over 150 thousand CSs to fulfil the Brazilian EV fleet demand by 2035 (ANFAVEA, 2021). Moreover, the insertion of these charging structures could cause equipment overload and power quality problems in the electric grid, such as voltage reduction. This situation is aggravated if fast charging stations (FCSs) are adopted, which have high charging power and behaves as centralized pulsating loads, which can lead to rapid changes in the load current and, consequently, voltages fluctuations, especially in weak grids (Nicholas & Hall, 2018) (Wang et al., 2021). Consequently, the electric distribution grid may need to be reinforced to sustain the power quality requirements, such as replacing cables with others of lower impedance or installing new assets.

On this matter, several research works have investigated the utilization of photovoltaics (PVs) and battery energy storage systems (BESSs) associated with FCSs as manners to reduce impacts in the electric grid (Tavakoli, et al., 2019) (Bouhouras, et al., 2019) (Mahmud et al., 2018) (Mahfouz & Iravani, 2019). New generators can locally provide the power

✉ José C. G. Andrade
jcga@unicamp.br

[1] Department of Energy and Systems, School of Electrical and Computer Engineering, The University of Campinas, Campinas, São Paulo 13083-852, Brazil

needed by the FCSs, which reduces the current from the substation and, consequently, the voltage drop along the feeder. If the time range of PV generation does not match the load profile of the FCSs, BESSs can store this energy to be used when needed.

However, just a few studies reported in the literature focus on the FCS's profitability and the economic viability of its integration with PVs and BESSs from the operator's perspective. In Liu et al. (2020) it is proposed a strategy of setting the limit of charging and discharging power of BESSs located in a CS with PVs installed based on load characteristics and the real time electricity price through an optimization process. The objective function of the optimization is the difference between the daily cost (CS and BESS costs divided per 365 days plus the daily electricity and maintenance costs) and the daily income (daily energy sold plus the vehicle charging service fee).

Some studies have considered stochastic modelling; however, their approaches are complex and difficult to apply in real distribution systems to evaluate charging events' impacts. In Moradzadeh and Abdelaziz (2020), a mixed integer linear programming (MILP) formulation is developed to determine the BESSs (type and capacity) and renewable energy sources, such as PVs and wind turbines, in order to minimize the energy cost associated with an FCS. However, implementation in real case studies of MILP optimization is complex due to the size of the problems.

Therefore, the goal of this paper is to analyze: (i) the time-of-use electricity tariff that maximizes the FCSs operators' profit under different circumstances; and (ii) the economic feasibility of PVs and BESSs integration with FCSs and how these technologies affect the FCS's profitability. Both aspects are analyzed using a stochastic model of charging events.

This paper is organized as follows: In Sect. 2, the EVs stochastic demand model is presented, highlighting how EVs' arrival instant and charging time are determined, and the EVs' demand curve construction algorithm is presented. In Sect. 3 is described the methodology for technical evaluation of impacts caused by the insertion of FCSs, PVs, and BESSs into the grid. In Sect. 4 are developed the economic methodologies, including approaches to size PVs and BESSs. Section 5 presents the data utilized in the analysis. In Sect. 6, both technical and economic results are presented. Conclusions are presented in Sect. 7.

2 Electric Vehicles Demand Modelling

To model the EV demand in FCSs, a load curve is built. Each point of this curve (also called multiplier) varies between 0 and the number of outlets that compose the FCS and represents the number of EVs charging during 15 min of a day. Initially, to create this curve, the number of EVs that visit the FCS in a day is specified along with another two parameters: the EV arrival instant and its charging time. The stochastic models are described in the subsections below.

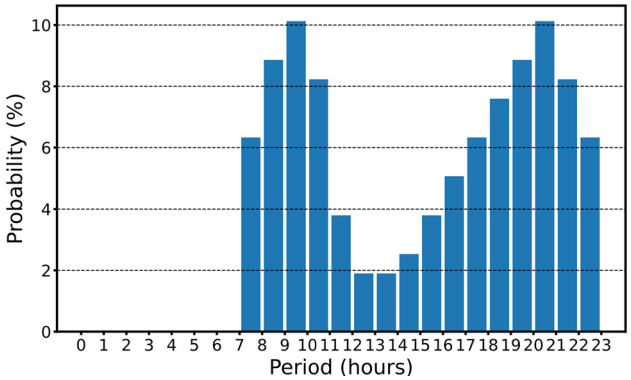

Fig. 1 Probability density function of vehicles arrival instant extracted from a real petrol station

2.1 Arrival Instant

The EV arrival instant is determined based on a probability density function (pdf) extracted from the utilization data of a convenience store of a real petrol station (due to the pattern resemblance between the petrol station and an FCS). The information about the utilization of this convenience store was extracted from the Popular Times section of Google Maps (Google, 2020) in April/2020 (Google updates this information regularly). For this paper, the data extraction was performed by scraping the HTML code of the web page. The probability density function built with the data extracted from Google Maps is depicted in Fig. 1.

2.2 Charging Time

In this part of the study, it was used the work developed in Jiang et al. (2014) to model the variables of interest. As established in Jiang et al. (2014), the EV charging time depends on the remaining energy in its battery, which is quantified by the State of Charge (SOC), and it is given in percentage (%).

To determine the SOC of each EV, it is necessary to know how much energy was spent, which is directly related to the distance traveled by the vehicle. A log-normal pdf of daily traveled distance, with zero probability for all negative distances, has been derived in Orr et al. (1982). The pdf is given as:

$$d(m) = \frac{1}{m\sigma\sqrt[2]{2\pi}} e^{\frac{-(\ln(m)-\mu)^2}{2\sigma^2}} \tag{1}$$

$$\mu = \ln(E[M]) - \frac{1}{2}\ln(1 + \frac{Var[M]}{E[M]^2}) \tag{2}$$

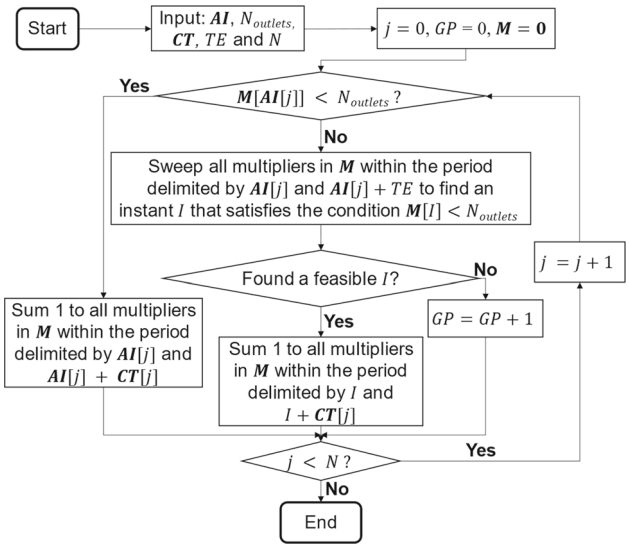

Fig. 2 Algorithm to determine the FCSs demand curve

$$\sigma^2 = \ln(1 + \frac{Var[M]}{E[M]^2}) \tag{3}$$

in which m is the daily distance driven, and $E[M]$ and $Var[M]$ are the mean value and variance of m.

Therefore, the SOC at the beginning of charging can be determined using the traveled distance by:

$$SOC = \begin{cases} \frac{R-m}{R} \times 100\%, \ 0 \leq m \leq R \\ 0, \ m \geq R \end{cases} \tag{4}$$

in which R is the all-electric range of the EV.

Finally, the charging time (CT) can be calculated using the previously determined SOC value and the EV nameplate parameters, *i.e.*, battery capacity and charger power, as follows:

$$CT = \frac{C(1 - SOC)DOD}{P\eta} \tag{5}$$

in which C is the battery capacity (kWh), P is the charger power (kW), DOD is the depth of discharge of the battery (%) and η is the efficiency of the charger (%).

2.3 Algorithm

Initially, the daily number of EVs that visit each FCS is specified (N); then an array with the arrival instant ($\boldsymbol{AI}$) and another with all charging times ($\boldsymbol{CT}$) of all EVs are built from the respective pdfs. These arrays are used as inputs in the demand curve construction algorithm shown in Fig. 2 alongside the FCS's demand multipliers curve ($\boldsymbol{M}$) (initially an array of zeros), the number of outlets in the FCS ($N_{outlets}$), the number of EVs that visited the FCS and a predetermined waiting time threshold (TE).

The FCS demand curve construction algorithm starts in the first EV ($j = 0$) and accesses its arrival instant ($\boldsymbol{AI}[j]$) and the multiplier value in the demand curve at this instant ($\boldsymbol{M}[\boldsymbol{AI}[j]]$). If the multiplier value is smaller than $N_{outlets}$, the demand curve ($\boldsymbol{M}$) is summed 1 between $\boldsymbol{AI}[j]$ and $\boldsymbol{AI}[j] + \boldsymbol{CT}[j]$ (charging time for the EV j). On the other hand, if the multiplier value is greater than $N_{outlets}$, all multipliers between $\boldsymbol{AI}[j]$ and $\boldsymbol{AI}[j] + TE$ are verified. If in one of these instants (l) the multiplier ($\boldsymbol{M}[I]$) is smaller than $N_{outlets}$, then 1 is summed to all multipliers between I and $\boldsymbol{I} + \boldsymbol{CT}[j]$. Nevertheless, if all multipliers are bigger than $N_{outlets}$, a "give-up" (GP) is registered, and the EV is not computed in the demand curve, *i.e.*, the EV does not recharge. This process is repeated to all the N EVs that visited the FCS.

3 Technical Analysis

The time-series power flow simulation is performed using OpenDSS (EPRI, 2016) associated with Python routines to assess the technical impacts caused by the insertion of FCSs in distribution systems and how the integration of PVs and BESSs into FCSs can affect the system. In this section is described the models for the FCS, PV, and BESS, including their controls, along with the technical metrics evaluated and the simulation algorithm.

3.1 Fast Charging Outlet Model

The FCSs are modeled as three-phase star-connected constant power loads, in which a single outlet has rated power of 50 kW and unitary power factor (Dharmakeerthi et al., 2012), (Egan et al., 2007). When inserted in LV systems, the FCSs are directly connected to the grid. However, if inserted in MV systems, the connection between the FCS and grid occurs through a distribution transformer, with sufficient rated power to supply all charging outlets that compose the FCS.

3.2 Solar Photovoltaic System

The PV model is made using the power expressions and the methodology presented in Atwa et al. (2009). The solar irradiation intensity throughout a day is approached as a beta function detailed in (6–9), where μ is the mean value and σ is the standard deviation.

$$\beta = (1 - \mu)(\frac{\mu(1 + \mu)}{\sigma^2} - 1) \tag{6}$$

$$\alpha = \frac{\mu\beta}{1 - \mu} \tag{7}$$

$$\Gamma(t) = \int_0^{\infty} x^{t-1} e^{x} dx \tag{8}$$

$$f_b(s) = \begin{cases} \frac{\Gamma(\beta)}{\Gamma(\alpha)\Gamma(\beta)} s^{(\alpha-1)}(1-s)^{(\beta-1)}, \ 0 \le s \le 1, \ \alpha \ge 0, \ \beta \ge 0 \\ 0, \ otherwise \end{cases} \tag{9}$$

The PV power curve ($\boldsymbol{P_{Sy}}$) is built using the solar irradiation curve (10–14):

$$Tc_y = T_A + s_{ay} \cdot \left(\frac{N_{OT} - 20}{0.8} \right) \tag{10}$$

$$I_y = s_{ay} \cdot (I_{SC} + K_i \cdot (T_C - 25)) \tag{11}$$

$$V_y = V_{OC} - K_v \cdot Tc_y \tag{12}$$

$$FF = \frac{V_{MPP} \cdot I_{MPP}}{V_{OC} \cdot I_{SC}} \tag{13}$$

$$P_{Sy} = N_{cells} \cdot FF \cdot V_y \cdot I_y \tag{14}$$

in which Tc_y is the solar cell temperature at y state, T_A is the ambient temperature (23 °C), s_{ay} is the mean solar irradiation at y state, N_{OT} is the solar cell nominal operation temperature, I_{SC} is the short-circuit current, K_i is the coefficient that relates current with temperature, V_y is the PV output voltage at y state, V_{OC} is the open-circuit voltage, P_{S_y} is the PV output power in y state, FF is the fill factor, N_{cells} is the number of solar cells in one PV and V_{MPP} and I_{MPP} correspond to voltage and current in the maximum power point, respectively.

3.3 Battery Energy Storage System

The battery model adopted throughout the studies is the $LiFePO_4$ battery, which is recommended for PV applications (Vega-Garita et al., 2019). Moreover, BESS is configured to operate with time triggers or following a shape.

3.3.1 Time Triggers without PVs

The charging and discharging time triggers used for BESSs associated with FCSs are determined as follows:

- The charging trigger is set in the off-peak period (21 h from one day to 18 h of the next day for FCSs installed in MV systems and 22 h from one day to 16 h of the next day for FCSs installed in LV systems employing White tariff), in a time that there is the minimum number of EVs plugged into the FCS's outlets. This is made aiming to recharge the batteries with the cheapest energy possible and avoid power demand violation (see Sect. 3.4 for details);
- The discharging trigger is set in the peak period (18 h to 21 h of the same day), in a time that there are EVs plugged into the FCS's outlets, aiming to reduce high-price energy consumption and the power demand.

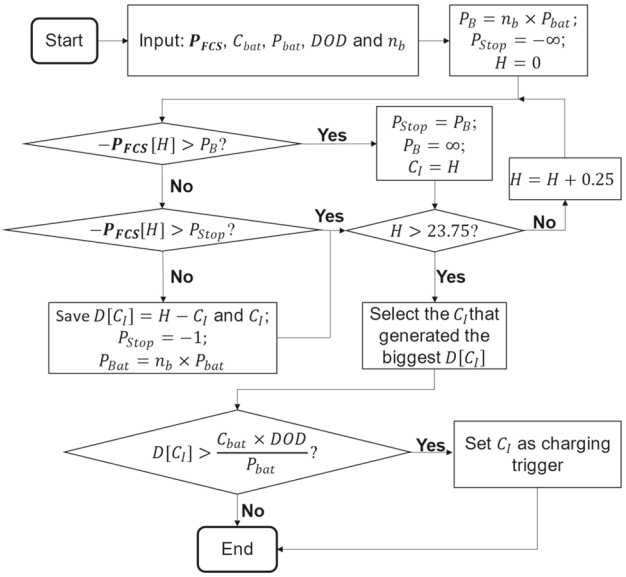

Fig. 3 Algorithm to determine the charging/discharging triggers of batteries adopted with PVs in FCSs

3.3.2 Time Triggers with PVs

The triggers used to control the BESSs (composed by n_b batteries) in FCSs with PVs are determined through the algorithm shown in Fig. 3. This algorithm receives the FCS power curve ($\boldsymbol{P_{FCS}}$), the battery's capacity in kWh (C_{bat}), the nominal power of the battery in kW (P_{bat}), the depth of discharge (DOD) and the number of batteries that will be inserted in the FCS (n_b) as inputs. In this algorithm is established the charging instants (C_I) only in moments when the power observed on the common coupling point between the grid and the FCS in a particular time ($\boldsymbol{P_{FCS}}[H]$) is negative and higher than the BESSs rated power (P_B). Furthermore, the charging trigger is set only if the power conditions mentioned above are sustained for a period ($D[C_I]$) longer than the time demanded to fully recharge the battery pack ($\frac{kWh \times DOD}{kW}$).

3.3.3 Shape

The curve is divided into two parts, one part for the peak hours and another for the off-peak period. This last one is built using the negative values of the PVs normalized power curve, while the first one is constructed filling all multipliers with one (to discharge all energy during high-price hours). Therefore, in the off-peak period, the battery charging power varies with the energy generated by the PVs; while, in the peak period, the battery pack discharges with nominal power.

Table 1 Statutory voltage limits in Brazil (ANEEL, 2021a)

Interval	LV costumers (pu)	MV costumers (pu)	Allowed time (%)
Proper	$0.92 \leq V \leq 1.05$	$0.93 \leq V \leq 1.05$	–
Precarious	$0.87 \leq V < 0.92$ or $1.05 < V \leq 1.06$	$0.90 \leq V < 0.93$	3
Critical	$V < 0.87$ or $V > 1.06$	$V < 0.90$ or $V > 1.05$	0.5

In this case, the curve is provided to OpenDSS instead of the time triggers.

3.4 Technical Metrics

The technical impacts caused by the insertion of FCSs in distribution systems are measured using the following metrics:

- *Steady-state Voltage:* according to Table 1 (ANEEL, 2021a);
- *Transformer Loading:* is considered overload if the power surpasses 150% of its nominal power for a period longer than 5% of the analyzed time (IEEE, 2012).
- *Line Loading:* is considered overloaded if the current surpasses the line ampacity for a period longer than 5% of the analyzed time (ABNT, 1985).

3.5 Algorithm

The methodology adopted to execute the electric grid simulations are based on the Monte Carlo method. In each iteration an FCS is installed in the electric grid, an EV demand curve for one day is created from the pdfs, PVs and BESSs are integrated into the FCS (for each case), a time-series power flow simulation is made, and the technical metrics are analyzed for each result. Each simulation represents 24 h of the day. A set of 100 Monte Carlo scenarios are simulated, enough to achieve the convergence following similar studies in the literature (Navarro-Espinosa & Ochoa, 2016) (Pinto et al., 2017).

4 Economic Analysis

Besides the technical impact assessment, cost mitigation is of great interest to FCSs operators. Therefore, a methodology is developed in this paper to assess how different time-of-use tariffs affects the FCSs costs in several scenarios. In the Brazilian case four different time-of-use tariffs are used depending on the grid voltage level:

- LV: Conventional and White, both monomials (*i.e.*, only charges by the energy consumed). However, the last one has different levels of price throughout the day;
- MV: Blue and Green, both binomials (*i.e.*, charges by the energy consumed and contracted demand). The first one has different prices for energy and power demand according to the period of the day, while the last one has different prices only for energy according to the periods of a day (single cost for power demanded).

In ANEEL, (2015) is defined the electric energy compensation system using net-metering, *i.e.*, all injected energy is discounted from the consumed energy for billing purposes. This standard is utilized in the economic evaluation of PVs and BESSs integration into FCSs.

4.1 Methodology

The economical assessment is made using the EV demand curve as input. Initially, the amount of energy consumed, and maximum power demanded are calculated. Therefore, the FCS's energy consumption cost is determined considering different time-of-use tariffs. Moreover, two methods to determine the ideal PV and BESS sizes are shown in this section.

4.1.1 Determination of Energy (Consumed and Generated)

The power curve is separated into different sections according to the number of levels of each tariff (Conventional has one level, Blue and Green have two levels and White has three levels). Then, the resulting arrays are divided into two arrays, one that contains the power consumed by the FCS (positive values), and another with the power injected by the FCS (negative values, considering PVs and/or BESSs integration, when integrated). The energy is calculated by integrating power demanded across the time for each array.

4.1.2 Power Demand

Another important aspect that composes the total cost of binominal tariffs is the contracted power demand. There is a fee to be paid if the maximum power withdrawn by an FCS exceeds 5% of the amount of power contracted (ANEEL, 2021b). The total amount paid for power demand is given by the sum of the contracted power demand price and the fee for surpassing the contracted power demand (15):

$$C_{DP} = P_{max} \cdot F_U - D_P \cdot (F_U - T_{DP});\ D_P \leq P_{max} \quad (15)$$

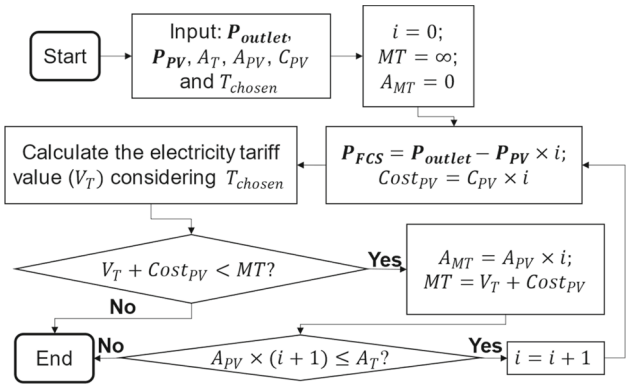

Fig. 4 Algorithm to determine the PV size

in which C_{DP} is the power demand total cost, P_{max} is the maximum power value consumed by the FCS, D_P corresponds to the contracted power demand, F_U is the fee rate for exceeding the contracted power demand, and T_{DP} is the contracted power demand tariff rate.

4.1.3 Tariff Equations

The time-of-use tariffs values are calculated as follows (ANEEL, 2021b):

$$T_B = TUSD_{Pp} \cdot PD_p + TUSD_{Pop} \cdot PD_{op} + TUSD_E \cdot EC_T + TE_p \cdot EC_p + TE_{op} \cdot EC_{op} \quad (16)$$

$$T_G = TUSD_P \cdot PD + TUSD_{Ep} \cdot EC_p + TUSD_{Eop} \cdot EC_{op} + TE_p \cdot EC_p + TE_{op} \cdot EC_{op} \quad (17)$$

$$T_W = TUSD_{Ep} \cdot EC_p + TUSD_{Eop} \cdot EC_{op} + TUSD_{Ei} \cdot EC_i + TE_p \cdot EC_p + TE_{op} \cdot EC_{op} + TE_i \cdot EC_i \quad (18)$$

$$T_C = TUSD_E \cdot EC + TE \cdot EC \quad (19)$$

in which T_B is the Blue tariff value, T_W is the White tariff value, T_G is the Green tariff value, T_C is the Conventional tariff value, $TUSD_{Px}$ is the contracted power demand cost rate, $TUSD_{Ex}$ is the energy availability cost rate, TE_x is the consumed energy cost rate, PD_x is the contracted power demand, and EC_x is the consumed energy in the x period, with x assuming p (peak hours), or op (off-peak hours) or i (intermediate hours–only for White tariff).

4.2 Determination of PV System Size

The PV system sizing is made according to the algorithm shown in Fig. 4. This algorithm calculates the ideal PV area to be installed in an FCS comparing the tariff costs, using the expressions (16–19), the type of tariff adopted (T_{Chosen}), the FCS and PVs power curves ($\boldsymbol{P_{outlet}}$ and $\boldsymbol{P_{PV}}$, respectively), the installation cost for one PV panel plus inverter (C_{PV}), the total area of the FCS (A_T) and the area occupied by a single PV panel (A_{PV}) as inputs. The total PV installation cost ($Cost_{PV}$) is given by the inverters and panels costs for each PV system (C_{PV}) multiplied by the number of panels installed (i) in an FCS.

In summary, the number of panels is increased, starting with zero, next, the total cost is calculated (electricity cost + equipment) and then compared to the minimum tariff value (MT). If a tariff value (V_T) obtained for an FCS with PVs summed with the PVs installation cost is smaller than the minimum tariff value obtained yet, the algorithm saves the minimum tariff value (MT) and the PVs installed area (A_{MT}). This search continues until the area reaches its maximum value (A_T).

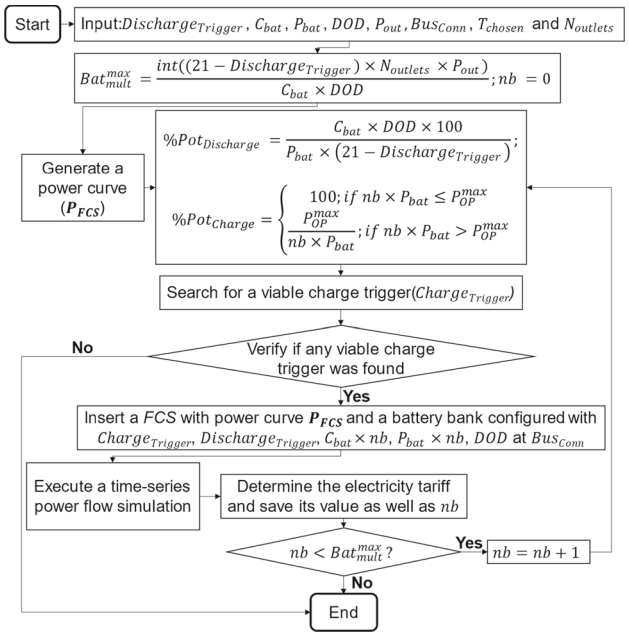

Fig. 5 Algorithm to determine size and time triggers of BESSs

4.3 Determination of BESS Size

To determine the BESS size configured with time triggers to be installed in the FCS (nb) without PV integration, the algorithm shown in Fig. 5 is utilized. This algorithm uses the discharge trigger ($Discharge_{Trigger}$), the capacity of the battery in kWh (C_{bat}), the nominal power of the battery (P_{bat}), the depth of discharge (DOD), the nominal power of a single charging outlet (P_{out}), the bus where the FCS is connected to the grid Bus_{conn}, the type of tariff adopted T_{chosen} and the number of outlets in the FCS ($N_{outlets}$). The

algorithm starts by calculating the maximum number of batteries that an FCS can support (Bat_{Mult}^{Max}) considering that the battery pack discharges during the peak period using the FCS nominal power. This number is determined using the $Discharge_{Trigger}$, $N_{outlets}$, P_{out}, C_{bat} and DOD.

In the algorithm is calculated the percentage of nominal power that the BESS charges ($\%Pot_{Charge}$) and discharges ($\%Pot_{Discharge}$). These parameters are calculated in such a way that the BESS cannot violate the off-peak power demand (P_{OP}^{max}) during charging moments and can discharge through the peak period considering P_{bat}. Moreover, the algorithm searches for a charge trigger for the BESS using the algorithm depicted in Fig. 3. The algorithm proceeds if a feasible charge trigger is found; otherwise, it ends.

Next, in the algorithm is inserted in the FCS connected at the bus Bus_{conn}, a BESS configured with the parameters calculated previously and then is executed a time-series power flow simulation, collecting the power curve at the common coupling point between the FCS and the distribution system.

Therefore, with this curve, the daily tariff value is calculated considering the time-of-use tariff adopted (T_{chosen}) in each scenario. Finally, the algorithm ends saving the number of batteries employed in the BESS and the obtained tariff value.

Nevertheless, if the batteries adopted in the FCSs are controlled through shape, an algorithm like the one depicted in Fig. 5 is used, with the batteries configured with shape information instead of time triggers. In this control scheme, the parameters Bat_{Mult}^{Max} and $\%Pot_{Discharge}$ are computed considering that the BESS starts to discharge at the beginning of the peak period and stops at the end of this period.

5 Case Study

The data utilized to execute the algorithms are presented in the following subsections.

5.1 Electric Grid

The electric grid used in the studies, shown in Fig. 6, is a distribution feeder (medium and low voltage explicitly modeled) located in the southeast region of Brazil, and it is composed of 142 three-phase distribution transformers, 2.815 electric lines, and 1.841 customers. Load profiles are provided by the local utility with 15 min resolution and different classes (residential, commercial, and industrial).

5.2 EVs and Charging Outlets

The data relating to the EVs specifications utilized to determine the SOC and charging time for each EV were extracted from a Nissan Leaf and are as follows: 240 km for the all-electric range; 40 kWh for the battery nominal capacity; 80% as DOD (Nissan, 2021). Additionally, 53.11 km and 32.83 km are used as the mean value and variance of the EV's daily traveled distances, respectively, (Jiang et al., 2014) to calculate the daily traveled distance for each EV.

Fig. 6 Geographic information of the distribution feeder

Regarding the FCS outlets, these structures are assumed to withdrawn 50 kW with an overall efficiency of 92.6% (Genovese et al., 2015).

5.3 PVs

The PV's power curve is built utilizing noon (0,5) as the mean hour value, and the solar irradiation is supposed to be relevant only in the period between 6:00 h (0,25) and 19:00 h (0,7916) (values in parentheses are hours normalized by a period of 24 h). These values are utilized to calculate the standard deviation, which is 3.82 h. Therefore, after the determination of α and β using Eqs. (7 and 8), the solar irradiation curve is constructed through the beta function.

The data required to calculate the expressions (9–13), shown in Table 2, were extracted from the Ulica UL-395 M-144 system (Ulica Solar, 2019). The unitary cost of the inverters and PVs adopted in the economic analysis are shown in Table 3 (NeoSolar, 2020a) (NeoSolar, 2020b).

Table 2 PVs parameters

$T_A(^oC)$	N_{OT}	$I_{sc}(A)$	$V_{OC}(V)$	$I_{MPP}(A)$	$V_{MPP}(V)$	$K_V(\%/^oC)$	$K_I(\%/^oC)$
25	45	10.31	49.1	9.83	40.2	− 0.29	0.049

Table 3 Cost of PV panel and inverter

Component	Cost (BRL/unit)
Ulica UL-395 M-144	1200
Hayonik 300 W Inverter	350

5.4 BESS

The $LiFePO_4$ batteries are modeled using the data presented in Table 4 (Tekenergy, 2020). The DOD, the nominal capacity and power of these batteries are used in the electric analyzes, while the number of life cycles and the battery price are employed in the economic analysis.

5.5 Tariff and demand fees

The tariff fees are extracted from the local utility, for the year 2020, and are shown in Table 5. The power demand fees for MV connection are shown in Table 6 (ANEEL, 2020).

5.6 Simulated Scenarios

In the technical analysis, two cases are studied. In one of these cases, the impact caused by the insertion of FCSs with one and five charging outlets in an LV system is analyzed, while in the other scenario the impact caused by the insertion of FCSs with those same features in an MV system is evaluated. The number of EVs visiting the FCS daily varies between 0 and 60 in both cases. Moreover, PVs are installed in a 2000 m^2 area and 4.8 kW by 7.2 kWh batteries are integrated into the FCSs to assess the potential of these technologies to reduce technical impacts in electrical distribution systems. The objective of these studies is to illustrate the technical impacts caused by FCSs. In the economic analysis, the FCSs always have one charging outlet; the remaining variables are in the same range as in the technical analysis.

Table 5 Tariff fees according to the voltage level

Voltage	Tariff	Period	Fee (BRL/MWh)
MV	Green	Peak	1,238.93
		Off-Peak	349.05
	Blue	Peak	525.87
		Off-Peak	349.05
LV	White	Peak	1,049.86
		Intermediate	673.71
		Off-Peak	474.37
	Conventional	All	550.2

Table 6 Power demand fees according to the voltage level

Tariff	Period	TUSD (BRL/kW)
Green	Peak	11.70
	Off-Peak	11.70
Blue	Peak	29.31
	Off-Peak	11.70

6 Results

In this section, the technical–economic impacts caused by the insertion of FCSs in electrical distribution systems are shown as well as the employment of PVs and BESSs.

6.1 Technical Assessment

The allocation of FCSs with one and five charging outlets in the LV grid cause violations, which are quantified by the proportion of customers (for voltage) or assets (for overloading) that violated these metrics, shown in Fig. 7. The results shown in Fig. 8 are obtained by installing the same FCSs in the MV grid.

The analysis of the results depicted in Fig. 7 reveals that voltage (percentage of customers with violation) is the most affected metric by the insertion of FCSs in LV systems. Additionally, the proportion of customers that violate this metric

Table 4 Battery parameters

Nominal capacity (kWh)	Nominal power (kW)	DOD (%)	Life cycles	Price (BRL)
7.2	4.8	80	6000	28,198

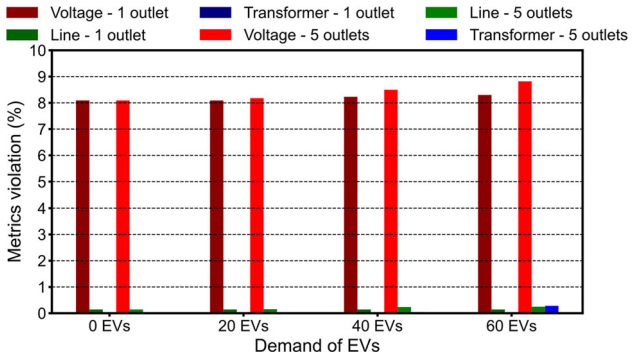

Fig. 7 Violation of metrics for the case of 1 and 5 charging outlets inserted in an LV system

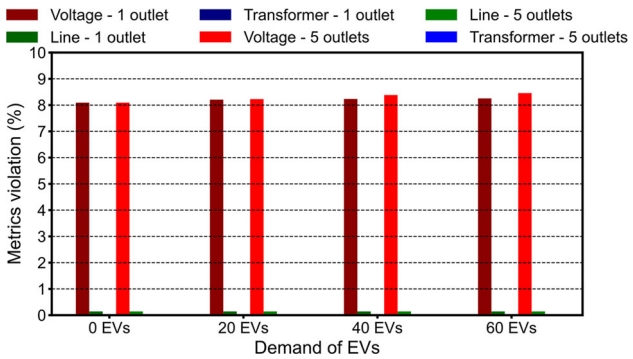

Fig. 8 Violation of metrics for the case of 1 and 5 charging outlets inserted in an MV system

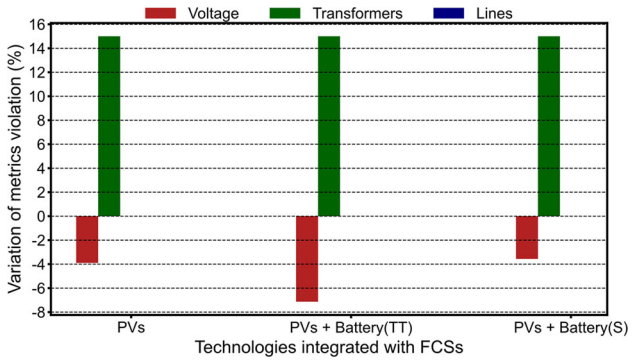

Fig. 9 Variation of violation with renewables integrated into the FCS

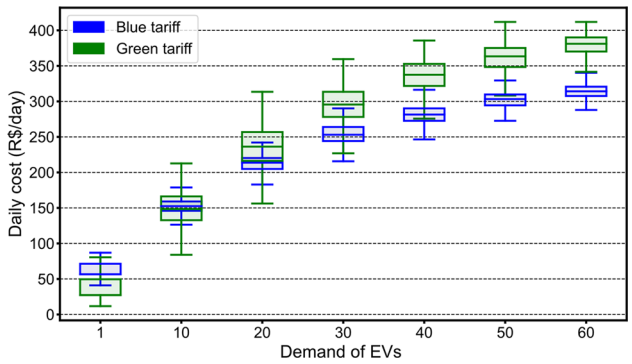

Fig. 10 Daily cost for the FCS considering Blue and Green tariffs according to the EV demand

increases with the number of EVs recharging and the number of outlets. From this same result, one can conclude that the allocation of an FCS with only one charging outlet is not likely to cause the overloading of lines and transformers. However, in the case of an FCS with five charging outlets, this impact is more likely to occur.

From Fig. 8, one can conclude that voltage is the most impacted metric by the insertion of an FCS in MV systems, which is similar to what happens in an LV system; however, with smaller variations. Also, overloadings are less likely to occur when the FCS is connected to the MV system.

The impacts caused by the integration of PVs and BESSs controlled with time triggers and shape in an FCS with 5 charging outlets in the LV system is analyzed. In this case, 60 EVs are visiting the station to recharge. The results are depicted in Fig. 9, which are given by the percentual variation over the case with 0 EVs shown in Fig. 7. As one can notice, the voltage violations are reduced by 4–7%, especially when PVs are combined with BESS. However, transformer overloading becomes 15% more likely, particularly because this evaluation is for an LV connection.

6.2 Economical Analysis

In this section is shown the economic results according to the equipment installed with the FCS.

6.2.1 FCSs without PVs and BESSs

To assess the energy and power consumption costs of the FCSs allocated in MV and LV systems, the algorithm presented in Sect. 4 is applied. The mean cost values employing the Conventional, White, Green, and Blue tariff are obtained through this process with 100 Monte Carlo simulations. The result for FCSs installed in MV and LV systems are shown in Figs. 10 and 11, respectively.

From Fig. 10, it is possible to conclude that the costs obtained employing the Blue tariff are lower than the costs obtained utilizing the Green tariff for all scenarios above 20 EVs, which suggests a higher influence of energy consumption rather than power demand on the final cost, particularly for higher usage of the FCS. From Fig. 11, one can conclude that the costs obtained employing the Conventional tariff are lower than the costs obtained utilizing the White tariff for all the analyzed scenarios.

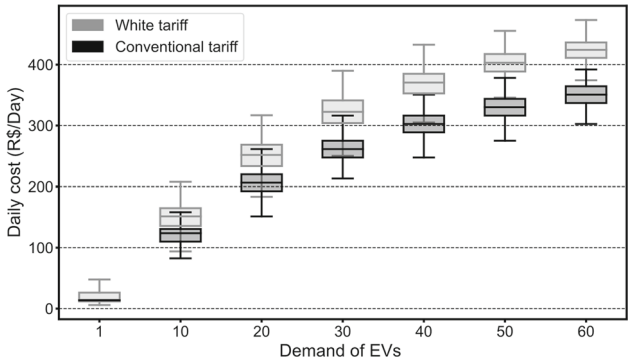

Fig. 11 Daily cost for the FCS considering Conventional and White tariffs according to the EV demand

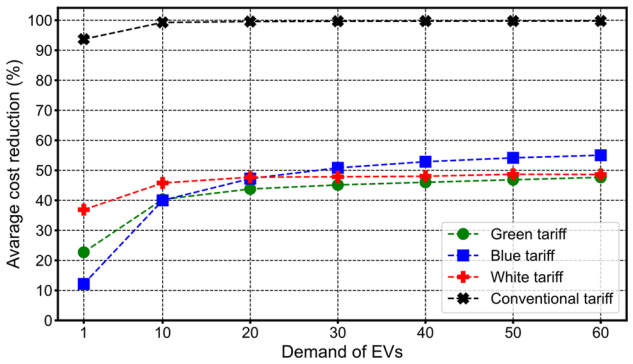

Fig. 12 Percentual reduction in cost by PVs integration

6.2.2 FCSs with PVs

To evaluate the effect of PV integration on the cost of power and energy consumption, PVs are allocated to the area that maximizes the costs reduction. The results, shown in Fig. 12, are given as the percentual reduction over the costs shown in Sect. 6.2.1.

The analysis of the results shown in Fig. 12 reveals that the FCS which adopted the Conventional tariff is the most benefited from PV integration, which diminished the FCS's cost to its daily availability cost. This occurs because in the LV system the FCS is only billed by energy consumption and as more energy is generated by the PV, the more it can reduce its cost.

Furthermore, by analyzing this same figure, one can conclude that the PVs integration also reduced significantly the costs related to power and energy consumption in the FCSs where White, Blue, and Green tariff were adopted (around 50% in cases of 20 or more EVs are recharging daily).

6.2.3 FCSs with BESSs

In this study, two forms of battery control, time triggers and shape, are adopted, and the effect on the FCS costs caused by each one of these control types are analyzed. In all the scenarios simulated, the results led to financial loss. This occurred because the BESS cost is not sufficiently low for this arbitrage scheme to become profitable (charging with cheap energy and discharging under higher prices).

6.2.4 FCSs with BESSs and PVs

In this analysis, the Conventional tariff is discarded because the PVs integration already reduced the FCS's energy and power consumption cost to its minimum allowable value.

BESSs Controled with Time Triggers The simulations with BESS controlled by triggers employed alongside PVs in FCSs led to the results shown in Tables 7, 8, and 9 for Green, White, and Blue tariffs, respectively. The values displayed on these tables are the percentage of scenarios in which the insertion of BESSs generated profit (P_P), the average percentual cost reduction (CR_P), the standard deviation of the percentual cost reduction (SD_{CR}) and the percentual cost reduction necessary for BESS employment be profitable (CR_N). Scenarios in which no viable charge trigger was found are not shown. In Table 8 and Table 9, for simplicity, only the results obtained for the installation of one and two batteries are displayed (others have lower profitability).

The analysis of the results from Table 7, for Green tariff, allows concluding that the insertion of one and two batteries for a daily demand of 10 EVs can be profitable ($CR_P > CR_N$). Additionally, by analyzing the P_P parameter, one can conclude that this value falls with the increase in the number of installed batteries for the same daily demand of EVs. This happens because the batteries are profitable only when they store the exceeding energy provided by the PVs. Also, due to the stochastic behavior of EV start charging it is difficult to determine the triggers, reducing the contribution of the BESS.

By analyzing the data displayed in Table 8, it is possible to conclude that the association of batteries with PVs has no economic viability in all the analyzed scenarios for White tariff ($CR_P < CR_v$). The same can be concluded by evaluating the content of Table 9, for the Blue tariff.

Batteries Controled with Shape The results achieved by the simulation of scenarios where FCSs have PVs and BESS controlled with shape are shown in Tables 10, 11, and 12 for Green, Blue, and White tariffs, respectively.

When the Green tariff is employed, the insertion of one and two batteries configured with shape is profitable for all the EVs demands analyzed. Moreover, one can conclude by observing the results in Table 10 that the parameter P_P is always lower than 50%, which suggests that there are some days when the BESS can reduce the FCS's costs expressively.

Table 7 Results for BESS configured with time triggers considering the Green tariff

D_{VEs}	N_B	P_P (%)	CR_p (%)	SD_{CR} (%)	CR_N (%)
10	1	56.00	4.47	2.21	4.27
	2	49.00	8.67	4.40	8.56
	3	49.00	12.05	6.58	12.84
20	1	49.00	2.50	0.91	2.74
	2	48.00	4.92	1.85	5.47
	3	48.00	7.08	2.60	8.24
	4	31.00	9.12	3.33	10.98
	5	31.00	10.98	3.93	13.72
30	1	52.00	1.94	0.82	2.24
	2	52.00	3.85	1.53	4.48
	3	40.00	5.67	2.27	6.75
	4	40.00	7.32	2.85	8.96
	5	29.00	8.91	3.41	11.21
	6	29.00	10.38	3.86	13.45
	7	27.00	11.74	4.17	15.68
40	1	36.00	1.71	0.67	2.05
	2	36.00	3.32	1.34	4.11
	3	36.00	4.87	1.97	6.15
	4	31.00	6.38	2.58	8.21
	5	31.00	7.79	3.07	10.26
	6	22.00	9.13	3.51	12.32
	7	22.00	10.41	3.88	14.36
	8	22.00	11.62	4.13	16.42
50	1	50.00	1.62	0.69	1.93
	2	34.00	3.10	1.25	3.85
	3	34.00	4.48	1.74	5.79
	4	17.00	5.72	2.13	7.70
	5	17.00	6.92	2.46	9.61
	6	17.00	8.08	2.78	11.56
	7	12.00	9.19	3.01	13.48
	8	12.00	10.28	3.20	15.42
60	1	59.00	1.70	0.66	1.86
	2	50.00	3.36	1.27	3.72
	3	50.00	4.95	1.87	5.58
	4	50.00	6.38	2.37	7.44
	5	34.00	7.71	2.81	9.30
	6	34.00	8.97	3.22	11.16
	7	22.00	10.05	3.37	13.02
	8	22.00	11.10	3.52	14.88

Table 8 Results for BESS configured with time triggers considering the White tariff

D_{VEs}	N_B	P_P (%)	CR_p (%)	SD_{CR} (%)	CR_N (%)
20	1	51.00	1.63	1.39	2.72
30	1	50.67	1.33	1.08	2.15
40	1	48.00	1.13	0.94	1.92
50	1	40.00	1.17	0.86	1.78
	2	40.00	2.09	1.62	3.56
60	1	48.66	1.06	0.82	1.73
	2	48.66	2.03	1.62	3.44

Table 9 Results for BESS configured with time triggers considering the Blue tariff

D_{VEs}	N_B	P_P (%)	CR_p (%)	SD_{CR} (%)	CR_N (%)
10	1	17.00	1.33	2.00	3.93
20	1	1.00	0.62	1.16	3.18

Table 10 Results for BESS configured with shape considering the Green tariff

D_{VEs}	N_B	P_P (%)	CR_p (%)	SD_{CR} (%)	CR_N (%)
10	1	49.33	4.81	2.11	4.11
	2	50.00	9.19	3.94	8.21
20	1	44.00	3.04	1.10	2.75
	2	44.33	6.00	2.05	5.53
30	1	51.33	2.53	0.87	2.26
	2	47.66	4.96	1.71	4.52
40	1	43.33	2.16	0.83	2.01
	2	44.00	4.28	1.55	4.02
50	1	39.00	2.07	0.70	1.90
	2	39.00	4.09	1.37	3.82
60	1	48.66	1.97	0.67	1.83
	2	36.33	3.90	1.33	3.67

However, the analysis of Table 11 reveals that the BESS are not able to generate profit in any of the studied cases for Blue tariff, even if the standard deviation is summed to the average percentual cost reduction. Additionally, in all scenarios, the parameter P_P is extremely low (below 10%). Furthermore, by analyzing the results displayed in Table 12, one can conclude that the insertion of BESS into FCSs employing the White tariff is economically unfeasible ($CR_P < CR_v$).

6.2.5 Sensitivity Analysis

In this part of the study, a sensitivity analysis of the total daily cost (energy + PVs + BESSs) is made considering an FCS with a demand of 40 EVs. This analysis consists in reducing the PV, BESS, and energy costs to percentages of 75 and 50% of the original value in scenarios where there is only PVs, PVs, and BESSs controlled with time triggers, and PVs and BESSs controlled with shape alongside an FCS. The results are depicted in Fig. 13.

The energy tariff reduction is the one that affects the total daily cost in all scenarios, since the energy cost, which represents a major part of the total daily cost, is directly related to the energy tariff. Also, in this situation, the gap between all tariffs is reduced, *i.e.*, the total costs tend to the same value regardless of the tariff chosen.

The PV cost reduction also has a strong effect on the total daily cost in all the scenarios studied since this reduction, the PV and inverter unitary cost, enables the FCS operator to adopt a higher number of PVs (larger area), which reduces the daily energy cost.

The BESS has a stronger effect on energy consumption rather than on power demand; because of this, customers that adopt tariffs with smaller differences in tariff fees (BRL/MWh) between peak and off-peak periods have a lower economic benefit. The FCSs that were more affected by

Table 11 Results for BESS configured with shape considering the Blue tariff

D_{VEs}	N_B	P_P (%)	CR_p (%)	SD_{CR} (%)	CR_N (%)
10	1	10.00	1.50	1.60	3.83
	2	7.00	2.89	3.02	7.63
20	1	4.00	0.72	1.30	3.29
	2	4.00	1.31	1.30	6.51
30	1	2.00	0.74	0.73	2.85
	2	2.00	1.35	2.25	5.75
40	1	2.00	0.64	1.13	2.76
	2	1.00	1.16	2.14	5.51

Table 12 Results for BESS configured with shape considering the White tariff

D_{VEs}	N_B	P_P	CR_p	SD_{CR}	CR_N
10	1	48.33%	1.72%	1.47%	2.49%
	2	33.00%	3.12%	2.69%	5.00%
20	1	48.00%	1.04%	0.80%	1.49%
	2	33.60%	1.91%	1.48%	2.98%
30	1	41.00%	0.80%	0.63%	1.21%
	2	41.00%	1.48%	1.16%	2.33%
40	1	46.00%	0.70%	0.56%	1.03%
	2	34.00%	1.30%	1.02%	2.03%
50	1	38.66%	0.58%	0.49%	0.93%
	2	38.66%	1.10%	0.93%	1.86%
60	1	43.00%	0.55%	0.50%	0.89%
	2	24.66%	0.98%	0.87%	1.77%

the BESSs cost reduction were the ones that adopted the green tariff (889.88 BRL/MWh difference between peak and off-peak period), and the white tariff (575.49 BRL/MWh difference between peak and off-peak period), while the FCS that adopted the blue tariff (176.82 BRL/MWh difference between peak and off-peak period) presented a small alteration in the total daily cost. Additionally, observing the graphic in the middle of Fig. 13, one can conclude that the battery cost reduction has a stronger effect in FCSs with BESS controlled by time triggers when its operator adopts the white tariff; observing the lower graphic of Fig. 13, it is possible to infer that the reduction in battery cost has a stronger effect in FCSs with BESS controlled by shape when the charging station adopts the green tariff.

7 Conclusion

In this paper, the technical impacts caused by the insertion of FCSs in LV and MV systems as well as the adoption of PVs and BESSs to reduce these impacts were studied. It was found that FCSs impacts, especially steady-state voltage, and its effects are enlarged when these structures are installed in LV systems. Moreover, it was found that the PVs and BESSs integration into FCSs can reduce voltage violation by 4–7%; however, care must be taken with transformer overloading when FCSs are installed in LV systems.

In the part that concerns the economic assessment of the FCSs operation, it was concluded through the analysis of the several time-of-use tariffs that the most beneficial ones are the Conventional tariff, for FCSs allocated in LV systems, and the Blue tariff, for FCSs installed in MV systems when no PV or BESS is installed.

The analysis of the cost reduction obtained with the adoption of PVs in the FCSs showed that PVs can significantly reduce the energy and power consumption costs of FCSs, being able to reduce the Blue tariff cost by 60%, and the Conventional tariff cost by almost 100% if sufficient installation area is provided. Additionally, the economic assessment of BESSs integration without PVs in FCSs revealed that this configuration is not profitable.

Finally, from the simulations where BESSs were associated with PVs in FCSs, it was found that the addition of batteries cannot reduce the FCSs costs enough to pay themselves for most of the EVs demands scenarios, except for

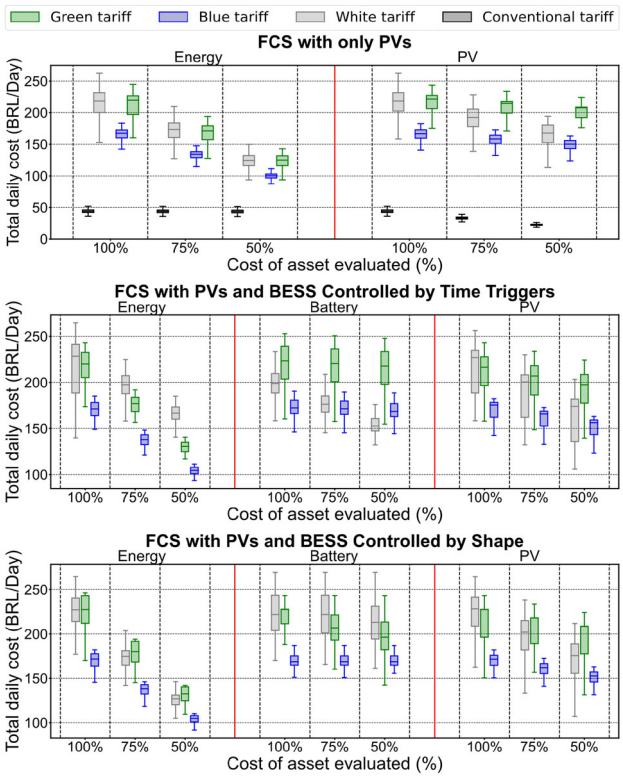

Fig. 13 Sensitivity analysis considering energy, battery, and PVs cost reduction for scenarios where FCS are implemented with PVs (upper figure), with PVs and BESS controlled by time triggers (figure in the middle), and with PVs and BESS controlled by shape (lower figure)

cases with significantly low demand, *i.e.*, BESS are profitable only when they store the exceeding energy provided by the PVs. Also, in this situation, the Green tariff has been shown to be the best choice.

From the sensibility studies, is worth noticing that reductions in energy, PV or BESS affect differently the total cost depending on the tariff chosen. When energy cost is reduced, the gap between all tariffs is also reduced. However, changing the cost of assets has more effect on White and Green tariffs, due to their energy cost difference (peak and off-peak values), depending on the BESS control type.

The studies shown in this paper aims to guide future analysis of FCS, PVs and BESSs assessments considering local market regulations because technical–economic results can significantly change depending on the country.

References

ABNT. (1985). NBR5422: Projeto de linhas aéreas de transmissão de energia elétrica.

ANEEL. (2015). Resolução normativa 687.

ANEEL. (2020). Resolução homologatória 2670.

ANEEL. (2021b). Resolução normativa ANEEL No 1000.

ANEEL. (2021a). Procedimentos de Distribuição de Energia Elétrica no Sistema Elétrico Nacional-PRODIST-Módulo 8: Qualidade da Energia Elétrica.

ANFAVEA. (2021). O caminho da descarbonização do setor automotivo no Brasil. https://www.bcg.com/pt-br/decarbonization-path-auto-sector-br.

Atwa, Y. M., El-Saadany, E. F., Salama, M. M. A., & Seethapathy, R. (2009). Optimal renewable resources mix for distribution system energy loss minimization. *IEEE Transactions on Power Systems, 25*(1), 360–70.

Bouhouras, A. S., Gkaidatzis, P. A., Panapakidis, I., Tsiakalos, A., Labridis, D. P., & Christoforidis, G. C. (2019). A PSO based optimal EVs Charging utilizing BESSs and PVs in buildings. In *2019 IEEE 13th International Conference on Compatibility, Power Electronics and Power Engineering*. Sonderborg, Denmark.

Dharmakeerthi, C. H., Mithulananthan, N., & Saha, T. K. (2012). Modeling and planning of EV fast charging station in power grid. In *2012 IEEE Power and Energy Society General Meeting*. San Diego, CA, USA.

Egan, M. G., O'Sullivan, D. L., Hayes, J. G., Willers, M. J., & Henze, C. P. (2007). Power-factor-corrected single-stage inductive charger for electric vehicle batteries. *IEEE Transactions on Industrial Electronics, 54*, 1217–1226.

EPRI. (2016). The open distribution system simulator (OpenDSS).

Genovese, A., Ortenzi, F., & Villante, C. (2015). On the energy efficiency of quick DC vehicle battery charging. *World Electric Vehicle Journal, 7*(4), 570–6.

Google. (2020). ampm - Google maps. https://goo.gl/maps/o8d8QjHN86jMzwBr7.

IEA. (2020). Tracking transport 2020. Paris.

IEA. (2021). Global energy outlook 2021. Paris.

IEEE. (2012). IEEE Std. C57.91: Guide for loading mineral-oil-immersed transformers and step-voltage regulators.

Jiang, C., Torquato, R., Salles, D., & Wilsun, X. (2014). Method to assess the power-quality impact of plug-in electric vehicles. *IEEE Transactions on Power Delivery, 29*(2), 958–965. https://doi.org/10.1109/TPWRD.2013.2283598

Liu, J., Cao, Y., & Gao, C. (2020). Multi-objective optimized configuration of electric vehicle fast charging station combined with pv generation and energy storage. In *2020 IEEE 3rd International Conference on Electronics Technology*, (pp. 467–473). Chengdu, China.

Mahfouz, M. M., & Iravani, M. R. (2019). Grid-integration of battery-enabled dc fast charging station for electric vehicles. *IEEE Transactions on Energy Conversion, 35*, 375–385.

Mahmud, K., Hossain, M. J., & Town, G. E. (2018). Peak-load reduction by coordinated response of photovoltaics, battery storage, and electric vehicles. *IEEE Access, 6*, 29353–29365.

Moradzadeh, M., & Abdelaziz, M. M. (2020). A new MILP formulation for renewables and energy storage integration in fast charging stations. *IEEE Transactions on Transportation Electrification, 6*, 181–198.

Navarro-Espinosa, A., & Ochoa, L. (2016). Probabilistic impact assessment of low carbon technologies in lv distribution systems. *IEEE Transactions on Power Systems, 31*, 2192–2203.

NeoSolar. (2020a). Painel Solar Fotovoltaico 395 W - Ulica UL-395–144. https://www.neosolar.com.br/loja/painel-solar-fotovoltaico-395w-ulica-ul-395m-144.html.

NeoSolar. (2020b). Inversor de 300 W 12/220V - Hayonik Onda Modificada. https://www.minhacasasolar.com.br/produto/inversor-de-tensao-300w-12-220v-onda-modificada-hayonik-pw-hay300-12v-220v-80151.

Nicholas, M., & Hall, D. (2018). Lessons Learned on Early Electric Vehicle Fast-Charging Deployments. *The International Council on Clean Transportation*.

Nissan. (2021). NISSSAN LEAF. https://www.nissan.com.br/veiculos/modelos/leaf.html.

Orr, J. A., Emanuel, A. E., & Oberg, K. W. (1982). Current harmonics generated by a cluster of electric vehicle battery chargers. *IEEE Transactions on Power Apparatus and Systems, PAS-101*(3), 691–700.

Pinto, Y., Trindade, F., Cebrian, J., & Teixeira, W. (2017). Investigation of infrastructural solutions to mitigate the impacts of EV recharging at LV networks. In IEEE PES Innovative Smart Grid Technologies Conference - Latin America (ISGT Latin America) (pp. 1–6). Quito, Ecuador: IEEE.

Ulica Solar. (2019). UL-395M-144 system. http://www.ulicasolar.com/modules_data/Datasheet%20for%20Mono%20385~395(Half-Cell).pdf.

Tavakoli, A., Saha, S., Arif, M. T., Haque, M. E., Mendis, N., & Oo, A. M. (2019). Impacts of grid integration of solar PV and electric vehicle on grid stability, power quality and energy economics: a review. *IET Energy Systems Integration, 2*(3), 243–60.

Tekenergy. (2020). Bateria Solar Litio Bateria Powerbox 48v Litio Lifepo4 7.2kwh Energia Solar Smart. https://loja.tekenergy.com.br/baterias?product_id=5645&limit=15.

Vega-Garita, V., Hanif, A., Nishant, N., Ramirez-Elizondo, L., & Bauer, P. (2019). Selecting a suitable battery technology for the photovoltaic battery integrated module. *Journal of Power Sources, 6*.

Wang, L., Qin, Z., Slangen, T., Bauer, P., & van Wijk, T. (2021). Grid impact of electric vehicle fast charging stations: trends, standards, issues and mitigation measures - an overview. *IEEE Open Journal of Power Electronics, 2*, 56–74. https://doi.org/10.1109/OJPEL.2021.3054601